Supplementary Information for

Maximizing the number of Rh^0-Rh^+ sites through metal dispersion control for the synthesis of higher alcohols from syngas

Ruyang Wang[1], Heng Cao[1], Peiyu Ma[1], Jun Bao[1,*]

[1]National Synchrotron Radiation Laboratory, Key Laboratory of Precision and Intelligent Chemistry, *i*ChEM (Collaborative Innovation Center of Chemistry for Energy Materials), University of Science and Technology of China, Hefei, Anhui 230026, China.

Corresponding authors:

*baoj@ustc.edu.cn. (J.B.)

Methods

Sample preparation

Synthesis of Ceria support: 1.39 g of $Ce(NO)_3 \cdot 6H_2O$ and 15.4 g of NaOH were dissolved in 8 and 56 mL of deionized water, respectively. The two solutions were mixed and stirred continually for 30 min. The mixed solution was then transferred into a Teflon-lined stainless-steel autoclave and hydrothermally treated at 100 ℃ for 24 h. The formed precipitation was centrifuged and rinsed with deionized water until the pH of the rinse water was about 7, and then rinsed three times with pure ethanol. The resulting sample was dried at 80 ℃ for 8 h and calcined in air at 400 ℃ for 4 h to obtain fresh CeO_2 support.[1, 2]

Synthesis of Rh/CeO_2 Catalysts: Rh/CeO_2 was prepared by incipient wetness impregnation method. Typically, the desired amount of $RhCl_3$ aqueous solution was added dropwise to CeO_2 powder, and the resulting slurry was stirred continually for 10 min. The obtained sample was dried at 60 ℃ for 8 h and then calcined in air at 450 ℃ for 4 h to obtain fresh Rh/CeO_2 catalysts. The Rh loading (1-8 wt. %) was adjusted by varying the concentration of $RhCl_3$ solution. The Rh/CeO_2 catalysts with different Rh loading are named xRh/CeO_2, where x represents the Rh loading. Prior to the reaction, the catalysts were reduced in a flow of H_2 (20 mL min^{-1}) at 400 ℃ for 4 h to obtain the reduced Rh/CeO_2 catalysts.

Characterizations

Brunauer-Emmett-Teller (BET) surface areas were tested on a Micromeritics Tristar II 3020 surface area and porosity analyzer. Raman spectra were performed on a LabRAM HR Evolution Raman spectrometer. Transmission Electron Microscopy (TEM) images were taken on a Hitachi H-7650 transmission electron microscope operating at an acceleration voltage of 100 kV. X-ray diffraction (XRD) patterns were recorded on a Philips X'Pert Pro Super diffractometer with Cu-Kα radiation (λ = 1.54178 Å). XPS measurements were performed on a Thermo ESCALAB 250Xi X-ray photoelectron spectrometer with Al Kα (hν = 1486.6 eV) as the exciting source. The high-angle annular dark-field scanning transmission electron microscope

(AC-HAADF-STEM) images were performed on a Themis Z spherical aberration corrected transmission electron microscope. The actual Rh loading in the catalyst was calculated based on the results of inductively coupled plasma atomic emission spectroscopy (ICP-AES) test. ICP-AES were performed on a Thermo Fisher iCAP 7400. The catalysts before calcination were dissolved in aqua regia for 12 hours, and the solution was diluted and filtered for ICP-AES test.

For the calculation of the total length of Rh-CeO_2 interface perimeter, it is assumed that the Rh particles in the catalysts are approximately hemispherical in shape. For a Rh crystal with a face centered cubic (FCC) structure, the atomic radius of the Rh atom is

$$r_{Rh}=\frac{\sqrt{2}\times 3\times d_{111}}{4\times\sqrt{3}}=0.135\ nm$$

where d_{111} is the interplanar spacing of the (111) crystal planes of Rh particles shown in the HAADF-STEM images. The total volume of 1 g of Rh crystal

$$V_{Rh}=\frac{N_A}{103}\times\frac{4}{3}\times\pi\times r_{Rh}^3\times\frac{1}{74.05\ \%}$$

where N_A is Avogadro constant, *74.05 %* is the space utilization rate of FCC densest stacking. The volume of individual Rh particle in the catalysts is

$$v_{Rh}=\frac{1}{2}\times\frac{4}{3}\pi R^3$$

where R is the radius of Rh particles shown in the HAADF-STEM images. In the catalyst containing 1 g of Rh, the total length of the Rh-CeO_2 interface perimeter is

$$L_{Rh\text{-}CeO_2}=\frac{V_{Rh}}{v_{Rh}}\times 2\pi R$$

After simplification, the total length of the Rh-CeO_2 interface perimeter in Rh/CeO_2 catalysts is

$$L_{Rh\text{-}CeO_2}=\frac{2.4\times 10^{11}}{R^2}=\frac{9.6\times 10^{11}}{D^2}\ (m/g_{Rh})$$

where D is the diameter of Rh particles shown in the HAADF-STEM images, and the unit of D is nanometer.

X-ray absorption fine structure (XAFS) spectra, including X-ray absorption near-edge structure (XANES) and extended X-ray absorption fine structure (EXAFS)

was performed at the BL11B beamline of Shanghai Synchrotron Radiation Facility (SSRF, Shanghai). A Si (311) monochromator was used for energy selection. The storage ring was operated at 3.5 GeV with an injection current of 200 mA. Rh foil was used as a reference sample and all X-ray absorption spectra were obtained in transmission mode. The raw XAFS data were processed using the Athena of the Demeter software package, and the fitting of EAXFS were implemented using the Artemis.

To characterize the reduced samples, the fresh Rh/CeO_2 catalysts were first loaded into a quartz tube and reduced in a tube furnace according to the reduction conditions. After the reduction is complete, both ends of the quartz tube were sealed and transferred to a glove box filled with high purity nitrogen. The sample was placed in a sealable sample holder specifically designed for the XPS testing to ensure that the sample were protected from air exposure during the test. For XAFS testing, the reduced samples were sealed in the glove box with special tape to avoid exposure to the atmosphere during testing.

Metal dispersion experiment, H_2 temperature-programmed reduction (H_2-TPR) and CO temperature-programmed desorption (CO-TPD) experiments were conducted on an automatic chemisorption equipment (Micromeritics, Model AutoChem II 2920). In the metal dispersion experiment, CO was used as the adsorbed molecule, and the ratio of Rh atoms to adsorbed CO molecules was assumed to be 1:1. After reduction, the catalyst was subjected to CO pulsing experiments, and the dispersion of Rh was calculated by calculating the number of Rh atoms exposed on the surface based on the consumption of CO. For H_2-TPR, the catalysts were first treated in a stream of He at 150 ℃ for 60 min. After cooling to room temperature in He, the gas flow was switched to H_2/Ar and purged continuously until the baseline was stabilized. The temperature was raised to 800 ℃ at a heating rate of 10 ℃/min, and the hydrogen consumption was monitored by a thermal conductivity detector (TCD). Before entering the TCD, the off-gas passed through a cold trap to remove the contained water. For CO-TPD, the reduced catalyst samples were first treated in a stream of He at 150 ℃ for 60 min, cooled to room temperature in He, then switched to CO/Ar and

held for 30 min. Subsequently, it was switched to He, and purged continuously until the baseline was stabilized. The temperature was then increased to 800 ℃ at a heating rate of 10 °C/min, and desorbed CO was monitored by a thermal conductivity detection (TCD) system.

H-D exchange experiment was carried out on a homemade micro-reactor, and a time-of-flight mass spectrometry was used to detect reactants and products in the exhaust gas. After the catalyst was loaded into the reactor, it was first heated up to 400 ℃ in 10% H_2/Ar and kept for 15 min to eliminate the slight oxidation caused by brief exposure of the samples to air. After the temperature of the reactor was cooled to 30 ℃, 10% H_2/Ar (30 ml/min) and 10% D_2/Ar (30 ml/min) were introduced into the reactor simultaneously, and intensity changes of H_2 (m/e = 2), D_2 (m/e = 4), and HD (m/e = 3) were recorded.

In situ diffuse reflectance infrared Fourier transform spectrum (DRIFTS) was collected on a Fourier transform infrared spectrometer (Thermo Fisher Nicolet iS50) equipped with a Harrick Praying Mantis DRIFT cell. Before testing, the samples were first reduced in a tube furnace according to the reduction conditions. The reduced samples were loaded into the DRIFT cell and then reduced in 10% H_2/Ar (20 ml/min) at 400 °C for 15 min to eliminate the slight oxidation caused by brief exposure of the samples to air, and then the experiment was performed. The DRIFTS were collected by accumulating 64 scans at a resolution of 8 cm^{-1} in Kubelka-Munk units. A series of *in situ* DRIFTS experiments were performed:

In situ CO DRIFTS at 25 ℃: For the CO adsorption DRIFTS experiment at 25 ℃, the sample was first pretreated in the infrared cell in Ar (30 ml/min) at 400 °C for 4 h, and then cooled to 25 °C to collect the background spectra. The feed gas was switched to 10% CO/Ar (15 ml/min) and the infrared spectra were collected until the CO adsorption reached saturation. Subsequently, the infrared cell was continuously purged by Ar to remove gaseous CO and unstable adsorbed CO, and the infrared spectra of chemisorbed CO species on the catalyst surface were obtained.

In situ CO-CO+H_2 DRIFTS at 320 ℃: The samples were pretreated under the same conditions and then cooled to 320 °C in Ar (30 ml/min) to collect background spectra.

Then, 10% CO/Ar (15 ml/min) was passed into the infrared cell, and the spectra were collected until the CO adsorption reached saturation. Subsequently, 10% H_2/Ar (30 ml/min) was introduced while maintaining a continuous flow of 10% CO/Ar (15 ml/min) to ensure that the ratio of H_2/CO is 2.0 in the gas stream. The infrared spectra was collected until the spectra stabilized.

In situ CO-H_2-D_2 DRIFTS at 125 ℃: The samples were pretreated under the same conditions and then cooled to 320 °C in Ar (30 ml/min) to collect background spectra. Then, 10% CO/Ar (15 ml/min) was passed into the infrared cell. After the CO adsorption was saturated, the feed gas was switched to 10% H_2/Ar (30 ml/min) and the infrared spectra were collected until the spectra stabilized. Subsequently, the feed gas was then switched to 10% D_2/Ar (30 ml/min) and the infrared spectra were collected. The total amount of Rh species contained in the catalysts with different loading filled into the reactor was equal to ensure comparability.

Computational Details

All the calculations were performed in the framework of the density functional theory with the B3LYP method. The 6-311g (d, p) basis set was used for C, O and H atoms and LANL2DZ basis set was used for Rh atom. The long-range van der Waals interaction was described by the DFT-D_3 approach. Rh_4 cluster was used to simulate the Rh nanoparticles. To account for the effect of CeO_2 on attracting electrons from Rh nanoparticles, we apply a one-unit positive charge to the Rh_4 cluster.

Catalyst Tests

The catalyst performance for HAS were evaluated in a stainless steel fixed-bed reactor equipped with a 9 mm inner diameter quartz-lined tube. Typically, a certain amount of catalyst was diluted with quartz sand and loaded into a quartz-lined tube. For catalysts with different Rh loading, the amount of catalyst and quartz sand were adjusted to ensure that the mass of Rh in the catalyst and the height of the catalyst bed were the same for each experiment. For example, 800 mg of catalyst and 1.2 g of

quartz sand were used for 1Rh/CeO_2; 100 mg of catalyst and 1.8 g of quartz sand were used for 8Rh/CeO_2.

Before the reaction, the catalyst was reduced in the reactor at 400 ℃ for 4 h with a H_2 flow rate of 20 mL min^{-1}, and then cooled to room temperature. Subsequently, the reactant gas mixture of 60% H_2/30% CO/10% N_2 was introduced into the reactor and then the reaction pressure and temperature were raised to set values. The standard reaction conditions are 320 ℃, 3.0 MPa, and a gas-hourly space velocity (GHSV) of 0.3 L mg_{Rh}^{-1} h^{-1}.

The off-gas was cooled in an ice-water bath to separate gas and liquid phases under reaction pressure. Two on-line gas chromatographs (Agilent GC-8860) were used to analyze the reaction products. One chromatograph equipped with a TCD was used to analyze H_2, N_2, CO, CH_4, and CO_2; another chromatograph was equipped with two FID detectors, one of which was used to analyze the gaseous hydrocarbon products such as CH_4, C_2H_6, etc., and the other was used to analyze the liquid oxygenated compounds. In calculating catalytic performance, CO conversion is defined as:

$$X_{CO}=1-\frac{A_{out}(CO)/A_{out}(N_2)}{A_{in}(CO)/A_{in}(N_2)}$$

where $A_{in}(CO)$ and $A_{in}(N_2)$ refer to the chromatographic peak area of CO and N_2 in the feed gas, and $A_{out}(CO)$ and $A_{out}(N_2)$ refer to the chromatographic peak area of CO and N_2 in the off-gas. Product selectivity is defined as:

$$Sel_{Ci}=\frac{N_{Ci}\times i}{\sum N_{Ci}\times i}$$

where N_{Ci} is the number of moles generated per hour of Ci product containing i carbon atoms. The ratio of non-dissociated and dissociated adsorbed CO is defined as:

$$\frac{\sum N_{Ci}\times i_n}{\sum N_{Ci}\times i_d}$$

where i_n is the number of carbon atoms in the Ci product that are attached to oxygen atoms, and i_d is the number of carbon atoms in the Ci product that are not attached to oxygen atoms.

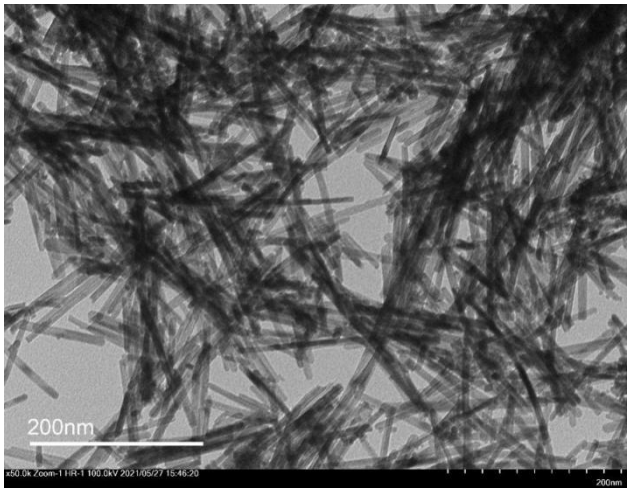

Fig. S1. TEM images of fresh CeO_2 support.

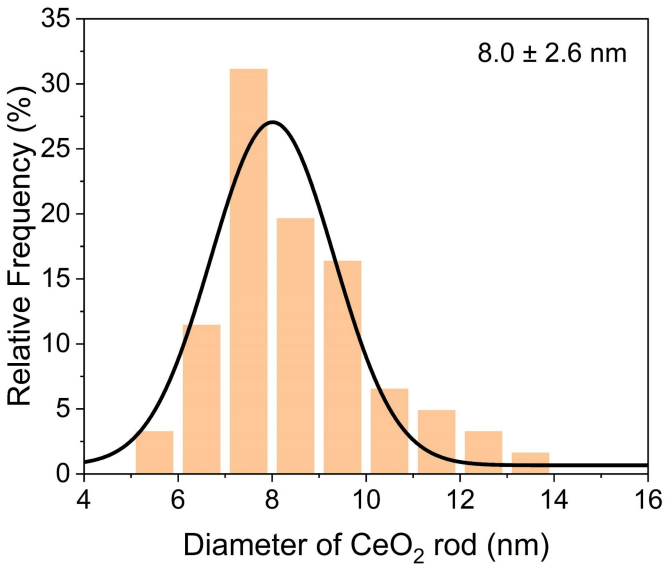

Fig. S2. Diameter distribution histograms of CeO_2 support.

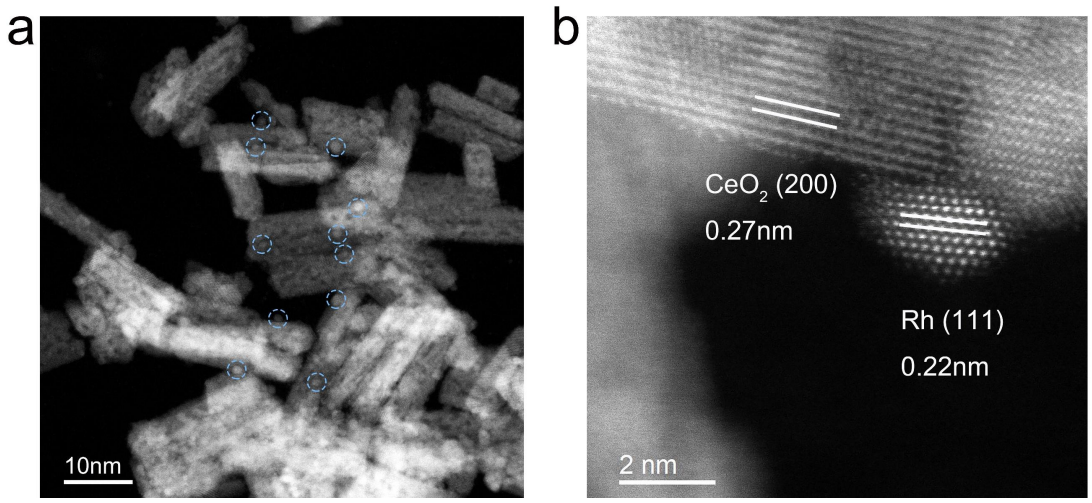

Fig. S3. a-b, HAADF-STEM images of reduced 8Rh/CeO_2 catalyst.

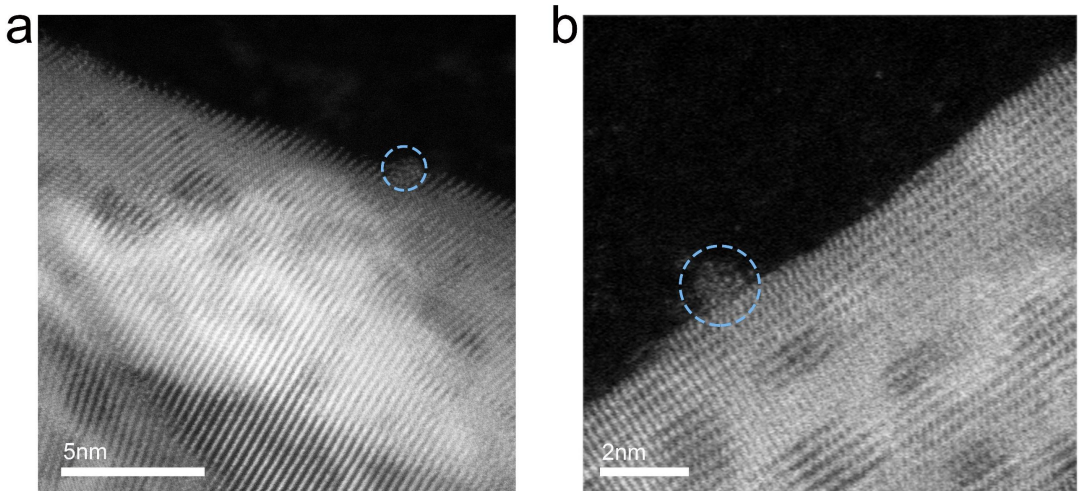

Fig. S4. a-b, HAADF-STEM images of reduced 1Rh/CeO_2 catalyst.

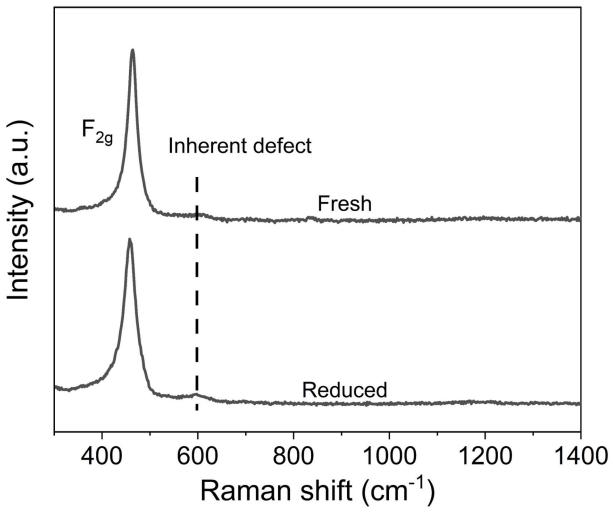

Fig. S5. Raman spectra of fresh and reduced CeO_2 support.

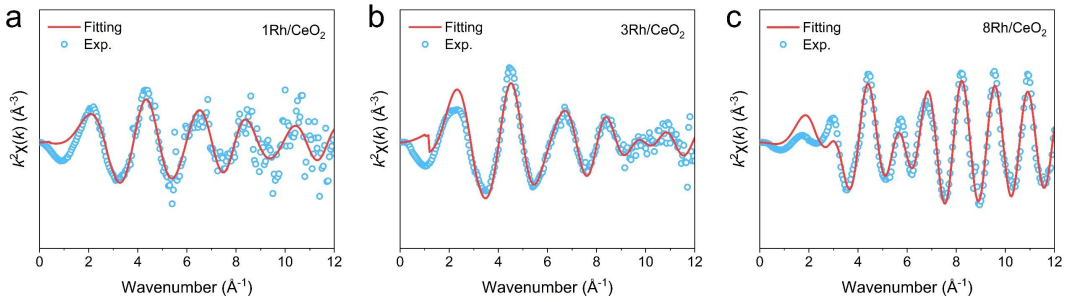

Fig. S6. a-c, Experimental and fitting EXAFS results in *k*-space of 1Rh/CeO_2 (a), 3Rh/CeO_2 (b), and 8Rh/CeO_2 (c).

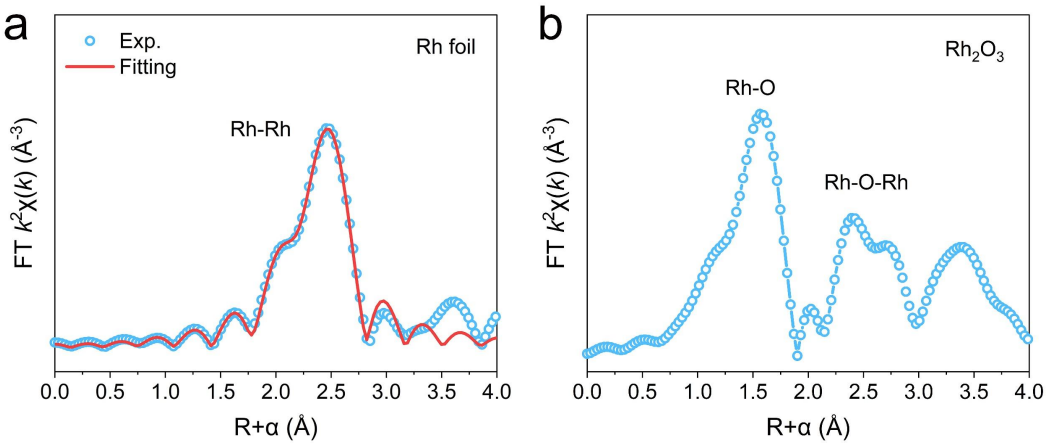

Fig. S7. (a) Experimental and fitting EXAFS results of Rh foil. (b) Experimental EXAFS results of Rh_2O_3.

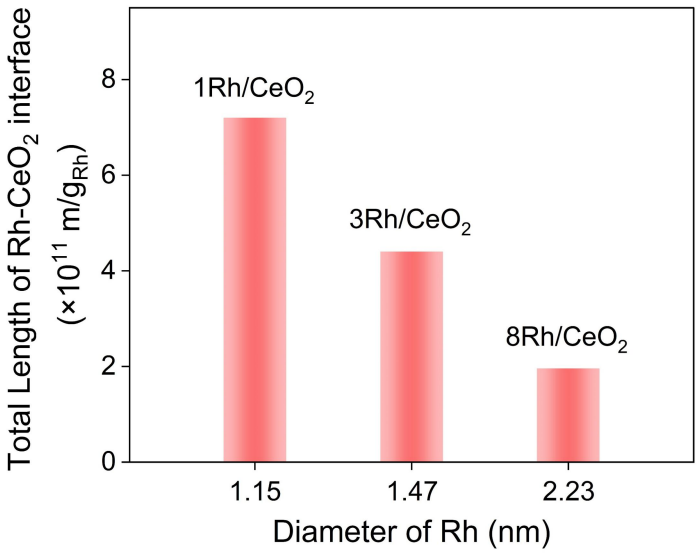

Fig. S8. The total length of Rh-CeO_2 interface perimeter in reduced Rh/CeO_2 catalysts with different size of Rh nanoparticles, calculated by assuming hemi sphericity of the Rh nanoparticles.

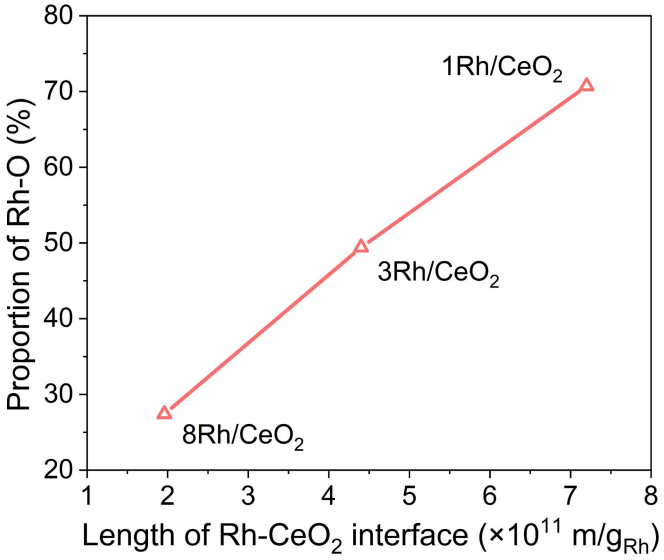

Fig. S9. The relationship between the total length of Rh-CeO_2 interface perimeter and the proportion of Rh-O obtained from linear combination fitting (LCF) results.

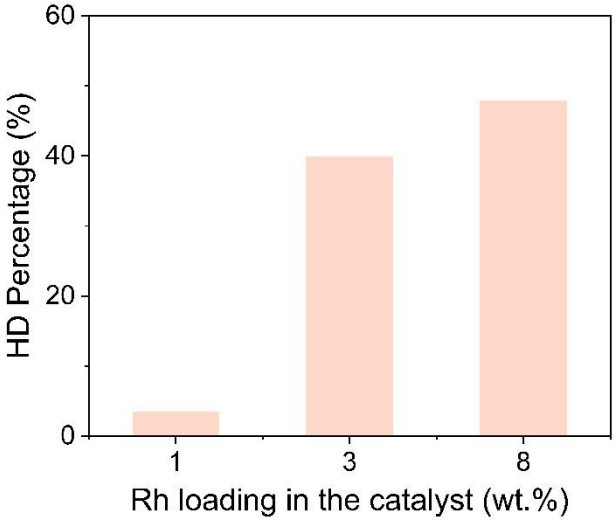

Fig. S10. H-D exchange results measured on Rh/CeO_2 catalysts.

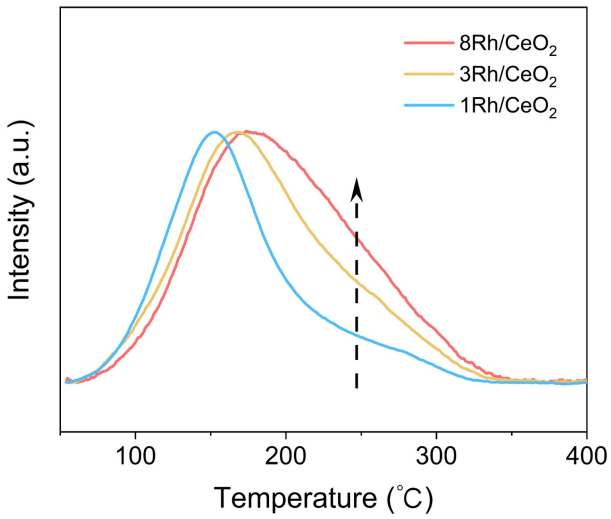

Fig. S11. CO-TPD curves of Rh/CeO_2 catalysts.

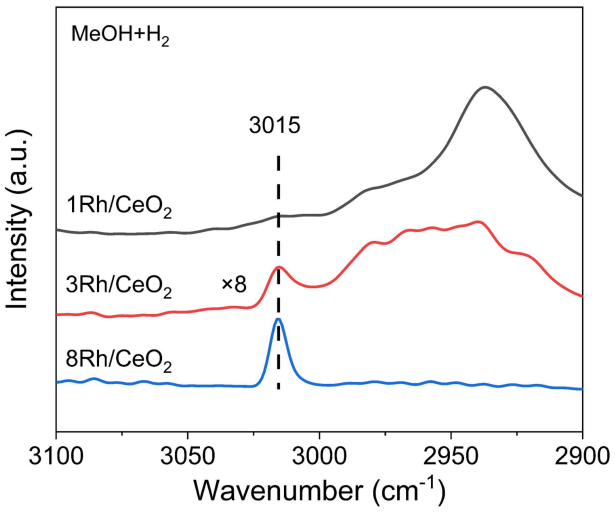

Fig. S12. *In situ* DRIFTS of Rh/CeO_2 catalysts at 320 ℃ after the $MeOH+H_2$ reaction was stable.

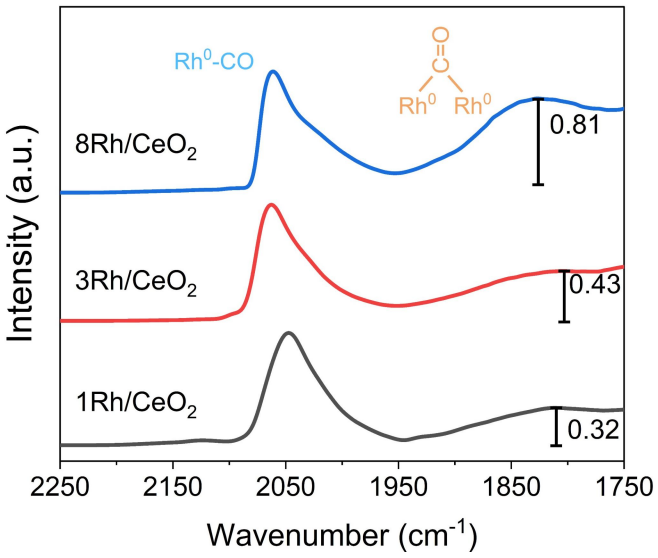

Fig. S13. DRIFTS of CO adsorption on Rh/CeO_2 catalysts after 2 hours of reaction.

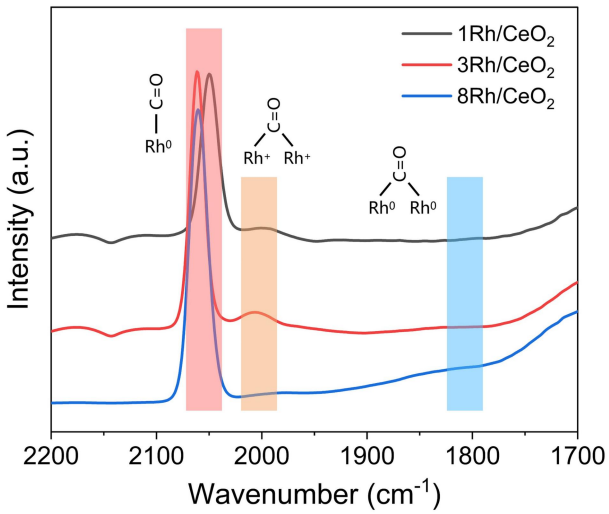

Fig. S14. *In situ* DRIFTS of CO adsorbed on reduced Rh/CeO_2 catalysts at 320 ℃.

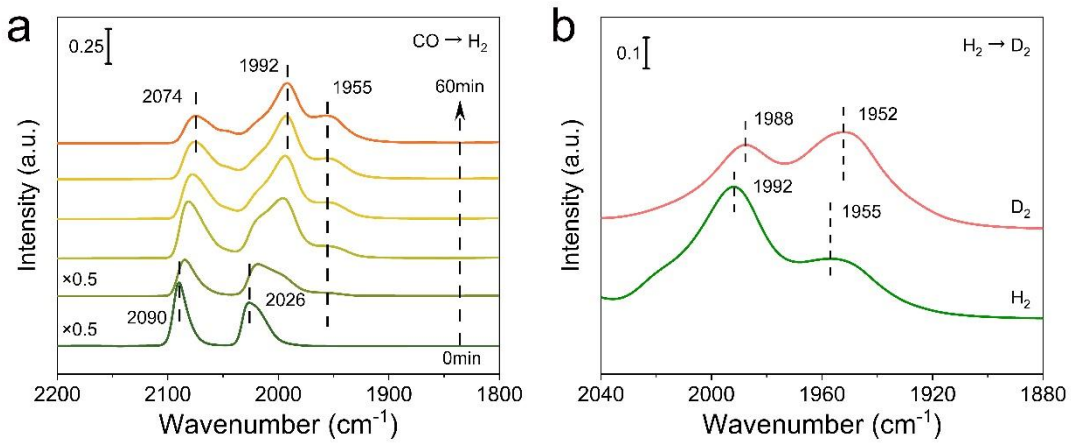

Fig. S15. Time-dependent *in situ* DRIFTS of 1Rh/CeO_2 at 125 ℃ after adsorbing CO to saturation (0 min), and then switching to H_2 (a). After the spectrum stabilizes, switched H_2 to D_2 (b).

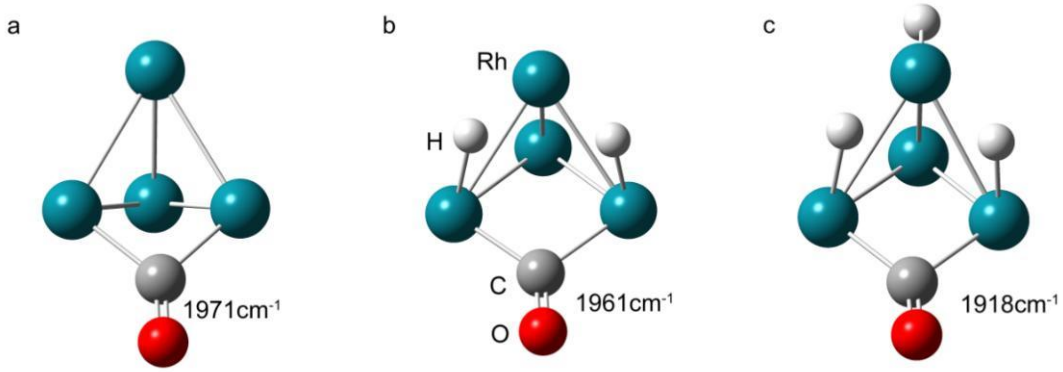

Fig. S16. The simulation of CO molecules adsorption on the theoretical structural model of Rh_4 (a), $Rh_2(RhH)_2$ (b) and $Rh(RhH)_3$ (c).

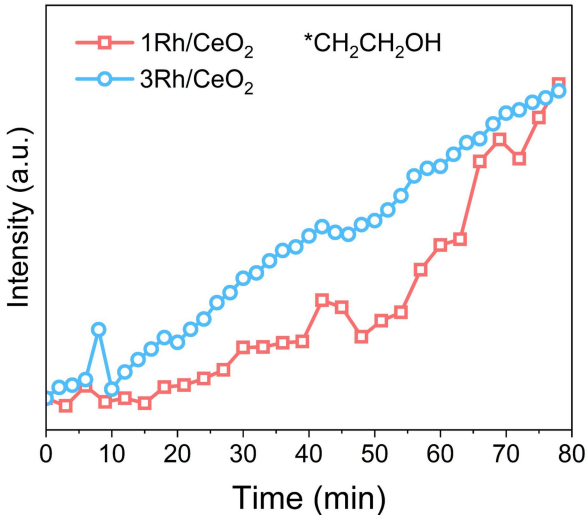

Fig. S17. The variation of normalized intensity of *CH_2CH_2OH intermediates over time observed in DRIFTS of 1Rh/CeO_2 and 3Rh/CeO_2.

Table S1. Brunauer-Emmett-Teller (BET) surface area of reduced Rh/CeO_2 catalysts with different Rh loading.

	$1Rh/CeO_2$	$3Rh/CeO_2$	$8Rh/CeO_2$
BET surface area (m^2/g)	76.62	78.48	76.48

Table S2. Rh loading in Rh/CeO_2 catalysts based on the results of ICP-AES.

	$1Rh/CeO_2$	$2Rh/CeO_2$	$3Rh/CeO_2$	$5Rh/CeO_2$	$8Rh/CeO_2$
Rh loading (wt. %)	0.94	1.88	2.81	4.84	7.56

Table S3. Metal dispersion measurement results of Rh/CeO_2 catalysts.

	$1Rh/CeO_2$	$2Rh/CeO_2$	$3Rh/CeO_2$	$5Rh/CeO_2$	$8Rh/CeO_2$
D_{Rh} (%)	59.99	35.50	26.78	26.08	21.55

Table S4. Quantitative calculation after peak fitting of the Raman spectrum.

		D_1/F_{2g}	D_2/F_{2g}	D_3/F_{2g}
$1Rh/CeO_2$	Calcined	0.04	1.06	0.04
	Reduced	0.14	0.78	0
$3Rh/CeO_2$	Calcined	0.02	2.29	0.20
	Reduced	0.31	1.39	0
$8Rh/CeO_2$	Calcined	0.01	4.10	0.24
	Reduced	0.82	1.97	0

Table S5. Linear combination fitting (LCF) results for Rh/CeO_2 catalysts.

	Rh^0 (%)	Rh-O (%)	R factor
$1Rh/CeO_2$	29.3	70.7	0.018
$3Rh/CeO_2$	50.6	49.4	0.013
$8Rh/CeO_2$	72.6	27.4	0.008

Table S6. The EXAFS fitting results of reduced Rh/CeO_2 catalysts.

Sample	Shell	CN [a]	R/Å [b]	$\sigma^2\times10^3$/Å^2 [c]	ΔE_0/eV [d]	R factor
Rh foil [e]	Rh-Rh	12.00	2.69 ± 0.01	3.5	4.7	0.004
$1Rh/CeO_2$ [f]	Rh-O	3.24 ± 1.50	2.04 ± 0.04	12	0.7	0.017
	Rh-Rh	0.33 ± 0.93	2.71 ± 0.17	4.8	-0.6	
$3Rh/CeO_2$ [g]	Rh-O	5.08 ± 2.19	2.05 ± 0.02	6.5	5.4	
	Rh-Rh	1.05 ± 0.35	2.68 ± 0.04	4.8	3.8	
$8Rh/CeO_2$ [h]	Rh-O	3.63 ± 1.08	2.04 ± 0.02	3.0	-0.8	
	Rh-Rh	5.29 ± 0.20	2.67 ± 0.01	4.8	-3.8	

[a] CN, coordination number.

[b] R, bonding distance.

[c] σ^2, the Debye-Waller factor (a measure of thermal and static disorder in absorber-scatterer distances).

[d] ΔE_0, the edge energy shift (the difference between the zero kinetic energy value of the sample and that of the theoretical model).

S_0^2, the amplitude attenuation factor, was fixed to 0.84 as determined from Rh foil fitting.

[e] Fitting range: $3.0 \leqslant k\,(/Å) \leqslant 12.35$ and $1.5 \leqslant R\,(Å) \leqslant 3.0$.

[f] Fitting range: $3.0 \leqslant k\,(/Å) \leqslant 11.20$ and $1.0 \leqslant R\,(Å) \leqslant 3.0$.

[g] Fitting range: $3.0 \leqslant k\,(/Å) \leqslant 11.30$ and $1.0 \leqslant R\,(Å) \leqslant 3.0$.

[h] Fitting range: $3.0 \leqslant k\,(/Å) \leqslant 12.40$ and $1.0 \leqslant R\,(Å) \leqslant 3.0$.

Table S7. Catalytic Performance of Rh/CeO_2 catalysts with different Rh loading.

Catalyst	X_{CO} (%)	Selectivity (C %)					Distribution of Oxygenates (C %)		
		CO_2	CH_4	MeOH	C_{2+}-Oxy	C_{2+}-H	CH_3OH	C_2-Oxy	C_{3-5}-Oxy
$1Rh/CeO_2$	2.6	37.0	25.2	21.6	12.3	3.9	63.6	13.3	23.1
$2Rh/CeO_2$	4.2	26.3	24.8	20.7	22.9	5.3	47.4	33.8	18.8
$3Rh/CeO_2$	5.7	20.7	33.0	13.1	25.1	8.1	34.4	55.0	10.6
$5Rh/CeO_2$	11.5	18.0	43.1	8.3	22.4	8.2	27.0	66.6	6.4
$8Rh/CeO_2$	17.7	17.1	51.6	4.4	19.3	7.6	18.6	76.6	4.8

Table S8. Catalytic performance of monometallic Rh catalysts on different supports.

Catalysts	X_{CO} (%)	Selectivity					ref
		CO_2	CH_4	MeOH	C_{2+}Oxy	C_{2+}H	
3Rh/CeO_2	5.7	20.7	33.0	13.1	25.1	8.1	This work
Rh/NCNT	23	46	33.2	1.0	13.1	21.8	[3]
Rh/TiO_2	0.8	2.5	58	6.8	20.4	8.6	[4]
Rh/WC	11.4	29.1	35.4	15.2	10.3	10.0	[5]
Rh/Al_2O_3	5.2	9.8	34.7	6.1	7.8	41.6	[6]
Rh/SiO_2	5	~0	70.2	1.4	15.0	11.6	[7]
Rh/SBA-15	68.8	62.8	36.5	0.4	0.11	—	[8]

Table S9. Catalytic Performance of 3Rh/CeO_2 catalyst in long-term test.

Time (h)	X_{CO} (%)	Selectivity (C%)					Distribution of Oxygenates (C%)		
		CO_2	CH_4	MeOH	C_{2+}-Oxy	$C_{2+}H$	CH_3OH	C_2-Oxy	C_{3-5}-Oxy
15	5.9	24.5	33.4	11.3	25.2	5.6	30.9	61.0	8.1
27	6.5	23.4	31.0	12.4	26.9	6.4	31.4	59.9	8.7
39	7.2	23.2	29.7	13.2	27.0	6.9	32.9	57.1	10.0
51	6.8	23.2	29.6	13.2	26.7	7.3	33.1	56.0	10.9
63	8.0	22.4	29.5	13.3	26.9	7.9	33.0	54.6	12.4
87	8.3	20.7	30.9	12.8	26.5	9.2	32.6	53.5	13.9
99	8.8	22.9	29.5	12.3	26.1	9.2	32.1	52.7	15.2
110	8.9	22.5	30.4	12.1	26.0	11.0	31.8	51.9	16.3

References

1 Jiang, F.; Wang, S.; Liu, B.; Liu, J.; Wang, L.; Xiao, Y.; Xu, Y.; Liu, X. *ACS Catal.*, 2020, **10**, 11493-11509.

2 Hu, Z.; Liu, X.; Meng, D.; Guo, Y.; Guo, Y.; Lu, G. *ACS Catal.*, 2016, **6**, 2265-2279.

3 Z. L. Xie, B. Frank; X. Huan,; R. Schlogl, Trunschke, *Catal. Lett.* 2016, **146**, 2417-2424.

4 A. Egbebi, V. Schwartz, S. H. Overbury, J. J. Spivey, *Catal. Today*, 2010, **149**, 91-97.

5 B. D. Won, H. Ham, J. M. Cho, J. B. Lee, C. U. Kim, H. S. Roh, D. J. Moon, J. W. Bae, *RSC Adv.*, 2016, **6**, 101535-101543.

6 Y. Chen,H. T. Zhang, H. F. Ma, W. X. Qian, F. Y. Jin, W. Y. Ying, *Catal. Lett.*, 2018, **148**, 691-698.

7 W. Mao, J. J. Su, Z. P. Zhang, X. C. Xu, W. W. Dai, D. L. Fu, J. Xu, X. G. Zhou, *Chem. Eng. Sci.*, 2015, **135**, 312-322.

8 G. C. Chen, C. Y. Guo, Z. J. Huang, G. Q. Yuan, Chem. *Eng. Res. Des.*, 2011, **89**, 249-253.